J. Fluid Mech. (1973), *vol.* 57, *part* 1, *pp.* 149–160
Printed in Great Britain

Supercritical flow in a divergent channel

By P. M. EAGLES
Department of Mathematics, The City University, London

(Received 24 April 1972)

For flow of a viscous fluid in a divergent channel of small angle it is shown that small disturbances to the basic Jeffery–Hamel flow may grow, according to nonlinear theory, to produce a secondary (supercritical) flow, in which the main flow winds from side to side in the channel and vortices form, with the whole pattern moving slowly downstream.

1. Introduction

We wish to consider small but nonlinear perturbations to the nearly parallel steady flow of a viscous incompressible fluid in a wedge of small divergence. Theory and calculations have been given by others for exactly parallel flow in a channel. The method developed by Stuart (1960) and Watson (1960) is based on a perturbation series in terms of an amplitude function of time which turns out to have magnitude proportional to $(R - R_c)^{\frac{1}{2}}$, where R_c is the critical Reynolds number beyond which the flow is unstable in the linear theory. The perturbation stream function may be expanded in a Fourier series whose first term is multiplied by a complex amplitude function $A(t)$, and it is found that

$$d|A|^2/dt = k_1|A|^2 + k_2|A|^4. \tag{1.1}$$

The constant k_1 is positive when the flow is *linearly* unstable, and negative when the flow is linearly stable. Now for Poiseuille flow, where the basic flow is exactly parallel and parabolic, Reynolds & Potter (1967) and Pekeris & Shkoller (1967) have shown that $k_2 > 0$ for a range of wavenumbers around the critical point. This gives no possibility of the so-called supercritical secondary flow developing.

The present work was undertaken mainly to show that $k_2 < 0$ for some flows of physical interest, namely for those Jeffery–Hamel flows appropriate to a divergent channel, and to examine the form of the flow for large time when $|A|$ approaches a constant.

There is some difficulty in applying Stuart's method to nearly parallel flow. In particular the boundary layer presents considerable difficulty. However, for flow in a wedge with small angle we are able to formulate the problem in a way that justifies proceeding as usual, except that the parabolic velocity profile of Poiseuille flow is replaced by a suitable Jeffery–Hamel profile. This will be explained in § 2.

We show by calculation that in fact the constant k_2 is negative for certain flows in channels. This allows the growth of small disturbances, as time increases, until they attain a constant amplitude; the perturbed flow after a long time takes

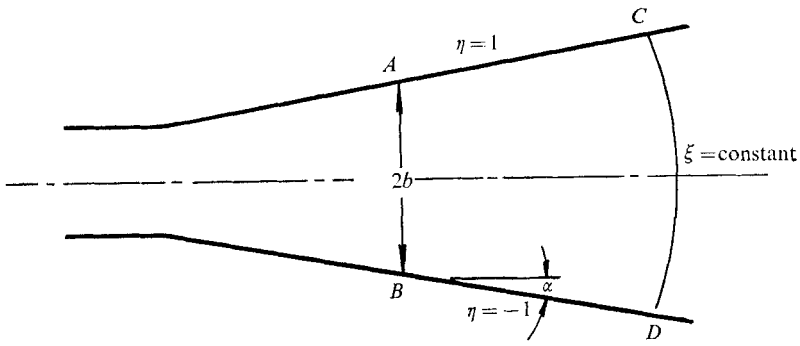

FIGURE 1. Illustration of the channel. The co-ordinates ξ and η are defined in (2.1).

a rather interesting form, illustrated in figure 4, with the main flow winding from side to side and a pattern of vortices appearing, the whole configuration moving slowly downstream.

2. Formulation of the basic problem

For definiteness we imagine the physical situation described below (though other interpretations of our work are possible). Let us suppose we have a long straight-walled divergent channel, $ACDB$ in figure 1. (This is smoothly attached to a curved-wall portion to the left and leads smoothly into a reservoir to the right.) We fix the points A and B at a distance $2b$ apart and imagine that we can swivel the walls about the points A and B to vary the divergence angle of the straight-walled part. Thus we have at our disposal the total volumetric flow rate $2M$ and the divergence angle 2α.

We introduce co-ordinates ξ and η defined by

$$r = (b/\alpha)\, e^{\alpha\xi}, \quad \theta = \alpha\eta, \tag{2.1}$$

where r and θ are the polar co-ordinates in the physical plane, with the origin at the point of intersection of CA and DB, such that the walls are given by $\theta = \pm\alpha$. We note that at A and B the value of ξ is $(1/\alpha)\ln(\alpha/\sin\alpha)$ and that this is approximately zero when α is small. We note also that $r \to \infty$ as $\alpha \to 0$ with ξ fixed, and this means that the origin tends to infinity to the left in figure 1. These co-ordinates are a special case of the more general co-ordinates introduced by Fraenkel (1963) in his study of channel flows.

Let $\Psi(\xi, \eta, t')$ denote the stream function, where t' is the time. The volumetric flow rate is $2M$, the kinematic viscosity is ν and the divergence angle is 2α. Upon setting $\Psi = M\psi$ and $t' = (b^2/M)\,\tau$ the vorticity equation reduces to the dimensionless form

$$\left[D^2 - Re^{2\alpha\xi}\frac{\partial}{\partial\tau} - R\left(\frac{\partial\psi}{\partial\eta}\frac{\partial}{\partial\xi} - \frac{\partial\psi}{\partial\xi}\frac{\partial}{\partial\eta}\right)\right][e^{-2\alpha\xi} D^2\psi] = 0, \tag{2.2}$$

where $R = M/\nu$ is the Reynolds number and where

$$D^2 \equiv \partial^2/\partial\xi^2 + \partial^2/\partial\eta^2. \tag{2.3}$$

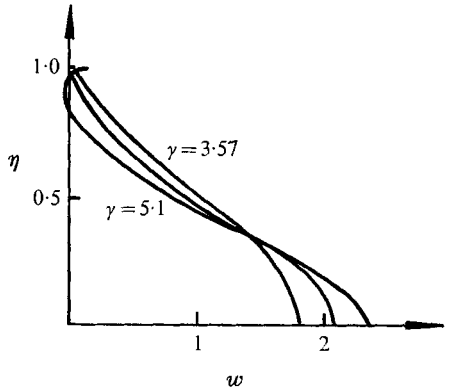

FIGURE 2. The Jeffery–Hamel velocity profiles $w(\eta;\gamma)$ for $\gamma = 3{\cdot}57$, $4{\cdot}71$ and $5{\cdot}10$. The centre of the channel is at $\eta = 0$ and the walls at $\eta = \pm 1$. The profiles are even in η.

The boundary conditions are that $\psi = \pm 1$ when $\eta = \pm 1$ and $\partial\psi/\partial\eta = 0$ when $\eta = \pm 1$.

There is a well-known family of exact, steady, ξ-independent solutions of (2.2), namely the Jeffery–Hamel solutions for flow in a wedge. Fraenkel (1962, 1963) has shown that a certain selection of these, symmetric in η and denoted by $G(\eta;R,\alpha)$, are appropriate to a symmetric channel of small and slowly varying wall curvature, the first approximation to the actual steady flow being given by the function G with the local α. The velocity profiles $g(\eta;R,\alpha) = dG/d\eta$ can easily be shown, from (2.2), to satisfy

$$g''' + 4\alpha^2 g' + 2\alpha R g g' = 0, \tag{2.4}$$

in which a prime denotes differentiation with respect to η. We shall later want to consider the limit $\alpha \to 0$ with $\gamma \equiv \alpha R$ fixed; and with the notation that $g(\eta;R,\alpha) \to w(\eta;\gamma)$ as $\alpha \to 0$ we see that

$$g(\eta;R,\alpha) = w(\eta;\gamma) + O(\alpha^2). \tag{2.5}$$

The numerical agreement is good. For example, with $\alpha = 0{\cdot}157$ and $R = 30$ Fraenkel's calculations show that g differs from w by less than 1 % at all values of η. The parameter $\gamma = R\alpha$ is restricted to a certain range for outward flows in a wedge. With $R = 10$, $0 < \gamma < 5{\cdot}05$; with $R = 20$, $0 < \gamma < 5{\cdot}40$; with $R = \infty$, $0 < \gamma < 5{\cdot}46$. The family of profiles $w(\eta;\gamma)$ contains Poiseuille flow ($\gamma = 0$), profiles with inflexion points ($\gamma > 1{\cdot}80$) and profiles with reversed flow near the walls ($5{\cdot}46 > \gamma > 4{\cdot}71$). Some of the profiles are illustrated in figure 2.

We wish to consider perturbations to the steady flow given by $G(\eta;R,\alpha)$ in a wedge. We therefore set

$$\psi = G(\eta;R,\alpha) + \psi_1(\xi,\eta,\tau;R,\alpha) \tag{2.6}$$

in (2.2) and find that

$$\frac{1}{R}\left\{\left(\frac{\partial}{\partial\xi} - 2\alpha\right)^2 + \frac{\partial^2}{\partial\eta^2}\right\} D^2\psi_1 - \left\{e^{2\alpha\xi}\frac{\partial}{\partial\tau} + g\left(\frac{\partial}{\partial\xi} - 2\alpha\right)\right\} D^2\psi_1 + \frac{d^2g}{d\eta^2}\frac{\partial\psi_1}{\partial\xi} + 2\alpha\frac{dg}{d\eta}\frac{\partial\psi_1}{\partial\eta}$$
$$= \left\{\frac{\partial\psi_1}{\partial\eta}\left(\frac{\partial}{\partial\xi} - 2\alpha\right) - \frac{\partial\psi_1}{\partial\xi}\frac{\partial}{\partial\eta}\right\} D^2\psi_1 \tag{2.7}$$

with boundary conditions

$$\partial\psi_1/\partial\xi = \partial\psi_1/\partial\eta = 0 \quad \text{when} \quad \eta = \pm 1. \tag{2.8}$$

We shall later use a perturbation scheme based on linear disturbance functions. Since the linear problem is rather complicated we first consider this, in order to decide on a suitable approximation to (2.7), for small values of α.

Let us first consider the limit of (2.7) as $\alpha \to 0$ with R fixed. It is easy to show that $g \to \frac{3}{2}(1-\eta^2)$, the Poiseuille flow profile for exactly parallel flow. If we discard the nonlinear terms and then set $\psi_1 = \phi(\eta)\, e^{ik(\xi - cr)}$ we obtain the well-known Orr–Sommerfeld problem

$$\left.\begin{aligned} (1/R)\,(\phi^{\mathrm{iv}} - 2k^2\phi'' + k^4\phi) &= ik\{(g_0 - c)\,(\phi'' - k^2\phi) - g_0''\phi\}, \\ \phi = \phi' &= 0 \quad \text{at} \quad \eta = \pm 1, \end{aligned}\right\} \tag{2.9}$$

in which $g_0 = \frac{3}{2}(1-\eta^2)$.

Now we consider the approximation as $R \to \infty$. At $R = \infty$ we lose the fourth derivative, so we have a typical singular perturbation problem for large values of R. In the Orr–Sommerfeld problem it is known from earlier work (Lin 1955; Eagles 1969) that there are regions of rapid variation with respect to η in the eigenfunction of (2.7). In particular $d\phi/d\eta = O(R^{\frac{1}{3}})$ in a region of width $O(R^{-\frac{1}{3}})$ around the point η_c, at which $w(\eta) = c$. Also $d\phi/d\eta = O(R^{\frac{1}{2}})$ in a wall layer. These two layers may coalesce under some circumstances. In any case, a proper asymptotic analysis which uses a stretched variable proportional to $(\eta - \eta_c)\, R^{\frac{1}{3}}$ near $\eta = \eta_c$ shows us that the correct first approximation *does* require the terms in $1/R$ on the left-hand side of (2.9), however large R may become. It is clear, also from a simpler point of view, that we must retain these terms in order to deal with the viscous boundary conditions. All this is well known, and we have outlined the above arguments to prepare the way for an approximation to (2.7) under a different limiting process.

In order to get away from the Poiseuille flow case we now consider the process $\alpha \to 0$ with γ fixed. The parameter $\gamma = R\alpha$ defines the members of the profile family $w(\eta;\gamma)$ of (2.5). Hence the terms in $1/R$ in (2.7) are formally of $O(\alpha)$ as $\alpha \to 0$, but an argument like the one above shows us that these terms must be retained, however small we take α, for a proper first approximation. The other terms of $O(\alpha)$ will all be discarded. We are thus led to the problem

$$\left.\begin{aligned} \frac{1}{R}(D^4\psi_1) - \left(\frac{\partial}{\partial\tau} + w\frac{\partial}{\partial\xi}\right) D^2\psi_1 + w''\frac{\partial\psi_1}{\partial\xi} &= \left(\frac{\partial\psi_1}{\partial\eta}\frac{\partial}{\partial\xi} - \frac{\partial\psi_1}{\partial\xi}\frac{\partial}{\partial\eta}\right) D^2\psi_1, \\ \partial\psi_1/\partial\xi = \partial\psi_1/\partial\eta &= 0 \quad \text{at} \quad \eta = \pm 1, \end{aligned}\right\} \tag{2.10}$$

in which $w = w(\eta;\gamma)$ with $\gamma = R\alpha$. Some further remarks on the validity of the approximation are made in § 5.

3. The expansion and amplitude equation

The aim here is to show that certain disturbance functions ψ_1 which are unstable according to linear theory will level off and attain a constant amplitude as time increases. The expansion method was suggested to the author by that of

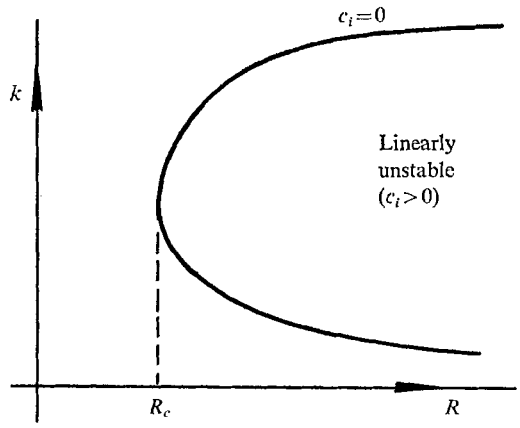

FIGURE 3. Schematic diagram of a typical curve of (linear) neutral stability. Here R is the Reynolds number and k is the wavenumber.

Matkowsky (1970), but since this work was completed Stewartson & Stuart (1971) have used an expansion of the same type for Poiseuille flow.

We first note that if we assume that

$$\psi_1 = \epsilon\phi(y)\, e^{ik(\xi-c\tau)} + O(\epsilon^2) \tag{3.1}$$

(where k is real and c is complex) and substitute this in (2.10) we obtain, from the $O(\epsilon)$ terms, the Orr–Sommerfeld problem

$$\left.\begin{aligned}(1/R)\,(\phi^{\mathrm{iv}} - 2k^2\phi'' + k^4\phi) = ik\{(w-c)\,(\phi'' - k^2\phi) - w''\phi\},\\ \phi = \phi' = 0 \quad \text{at} \quad \eta = \pm 1.\end{aligned}\right\} \tag{3.2}$$

If we fix γ, which specifies the profile $w(\eta;\gamma)$, then for given values of R and k we may solve for the eigenvalue† c. Curves in the R, k plane on which the imaginary part of c is zero are the neutral curves for stability, and some of these have been calculated by Eagles (1966). A typical neutral curve is shown in figure 3.

For any given value of k, if we increase R from zero, we find that the imaginary part of c will initially be negative and become positive when $R > R_1(k)$. Thus if $c = c_r + ic_i$ we have

$$c_i = 0 \quad \text{at} \quad R = R_1(k). \tag{3.3}$$

Hence the linear disturbance of given wavenumber k becomes unstable for sufficiently large R (with k limited to a certain range). Therefore for $R > R_c$ we shall expect a physical disturbance to grow initially, since it will have, in general, components of the type (3.1) which are unstable. However, a pure disturbance like (3.1) will grow only when $R > R_1(k)$. In order to examine the nonlinear effects we fix k and use the small parameter ϵ, where

$$\epsilon^2 = 1/R_1 - 1/R, \quad k \text{ fixed}. \tag{3.4}$$

It is possible to obtain a consistent expansion as follows. We define a new 'slow' time variable

$$t = \epsilon^2\tau, \tag{3.5}$$

† We refer here to that value of c with greatest imaginary part.

and introduce the notation

$$E = e^{ik(\xi-\lambda\tau)}, \tag{3.6}$$

where $\lambda(k)$ is the real part of c at $R = R_1(k)$ (on the neutral curve). We now set

$$\psi_1 = \epsilon(\phi_{11}E + \phi_{1,-1}E^{-1}) + \epsilon^2(\phi_{22}E^2 + \phi_{20} + \phi_{2,-2}E^{-2}) + \epsilon^3(\phi_{33}E^3 + \phi_{31}E^1 + \phi_{3,-1}E^{-1} + \phi_{3,-3}E^{-3}) + \ldots, \tag{3.7}$$

where each of the functions ϕ_{mn} depends only on η and on the 'slow' time t; thus

$$\phi_{mn} = \phi_{mn}(\eta, t). \tag{3.8}$$

It is clear that $\phi_{m,-n} = \overline{\phi}_{mn}$, the complex conjugate of ϕ_{mn}, and that ϕ_{m0} is real. We note also that $\partial/\partial\tau$ in (2.10) operates on both E^n and $\phi_{mn}(\eta, t)$ in a typical term of (3.7), but that its operation on ϕ_{mn} produces a multiplying factor of ϵ^2. Hence a term in $\partial\phi_{11}/\partial t$ occurs at order ϵ^3. If we equate the coefficients of powers of $\epsilon^m E^n$ we obtain partial differential equations for the ϕ_{mn}. With the notation

$$L^{(n)} \equiv \frac{1}{R_1}\left(\frac{\partial^4}{\partial\eta^4} - 2n^2k^2\frac{\partial^2}{\partial\eta^2} + n^4k^4\right) - ikn(w-\lambda)\left(\frac{\partial^2}{\partial\eta^2} - n^2k^2\right) + iknw'' \tag{3.9}$$

the equations are as follows.

$$L^{(1)}\phi_{11} = 0. \tag{3.10}$$

$$L^{(2)}\phi_{22} = \tfrac{1}{2}M(1, 1, \phi_{11}, \phi_{11}). \tag{3.11}$$

$$L^{(0)}\phi_{20} = M(1, -1, \phi_{11}, \phi_{1,-1}). \tag{3.12}$$

$$L^{(1)}\phi_{31} = \left(\frac{\partial^4}{\partial\eta^4} - 2k^2\frac{\partial^2}{\partial\eta^2} + k^4\right)\phi_{11} + \left(\frac{\partial^2}{\partial\eta^2} - k^2\right)\frac{\partial\phi_{11}}{\partial t} + M(1, 0, \phi_{11}, \phi_{20}) + M(-1, 2, \phi_{1,-1}, \phi_{22}). \tag{3.13}$$

Here the terms of the form $M(p, q, \phi_{jk}, \phi_{lm})$ are the nonlinear terms. Explicitly, we define

$$N(p, q, f, g) = ikq\frac{\partial f}{\partial\eta}\left(\frac{\partial^2 g}{\partial\eta^2} - q^2k^2g\right) - ikpf\left(\frac{\partial^3 g}{\partial\eta^3} - q^2k^2\frac{\partial g}{\partial\eta}\right), \tag{3.14}$$

where $f = f(\eta, t)$ and $g = g(\eta, t)$; then M is defined by

$$M(p, q, f, g) = N(p, q, f, g) + N(q, p, g, f). \tag{3.15}$$

The right-hand side of each of (3.9)–(3.13) depends only on functions from earlier equations in the set. The left-hand sides consist essentially of the Orr–Sommerfeld operator applied to the function ϕ_{mn} except that k is replaced by nk in each case, and t appears as a parameter in the ϕ_{mn}.

The boundary conditions

$$\phi_{mn} = \partial\phi_{mn}/\partial\eta = 0 \quad \text{at} \quad \eta = \pm 1 \tag{3.16}$$

are imposed, and we notice that the total volumetric flow rate and the Reynolds number are left exactly as they were for the steady flow. However, it is known from other work that the *even* eigenfunctions of the linear problem are the most unstable, and we therefore choose ϕ_{11} to be even in η. This is then the eigenfunction associated with that (most unstable) value of c which we discussed earlier in

connexion with the neutral stability curves. By examining (3.10)–(3.12) it is now easy to see that ϕ_{20} and ϕ_{22} are odd while ϕ_{31} is even. The even solution to (3.10) is

$$\phi_{11} = A(t) f_{11}(\eta), \tag{3.17}$$

where $A(t)$ is some function of t and

$$\left.\begin{aligned} L^{(1)} f_{11}(\eta) &= 0, \\ f_{11} = f''_{11} = 0 \quad \text{at} \quad \eta = 0; \quad f_{11} &= f'_{11} = 0 \quad \text{at} \quad \eta = 1. \end{aligned}\right\} \tag{3.18}$$

This is just the Orr–Sommerfeld problem with $c = \lambda =$ real and with the appropriate R_1. We can solve for $f_{11}(\eta)$ and proceed.

We now work just on the interval $0 \leqslant \eta \leqslant 1$ and find from (3.11) and (3.17) that

$$\phi_{22} = A^2(t) f_{22}(\eta), \tag{3.19}$$

where the problem for $f_{22}(\eta)$ is

$$\left.\begin{aligned} L^{(2)} f_{22}(\eta) &= \tfrac{1}{2} M(1, 1, f_{11}, f_{11}), \\ f_{22} = f''_{22} = 0 \quad \text{at} \quad \eta = 0; \quad f_{22} &= f'_{22} = 0 \quad \text{at} \quad \eta = 1. \end{aligned}\right\} \tag{3.20}$$

Similarly

$$\phi_{20} = A(t)\overline{A(t)} f_{20}(\eta), \tag{3.21}$$

where the problem for $f_{20}(\eta)$ is

$$\left.\begin{aligned} L^{(0)} f_{20}(\eta) &= M(1, -1, f_{11}, f_{1,-1}), \\ f_{20} = f''_{20} = 0 \quad \text{at} \quad \eta = 0; \quad f_{20} &= f'_{20} = 0 \quad \text{at} \quad \eta = 1. \end{aligned}\right\} \tag{3.22}$$

The functions $f_{22}(\eta)$ and $f_{20}(\eta)$ are uniquely determined by (3.20) and (3.22).

The problem for $\phi_{31}(\eta, t)$ is obtained from (3.13) and is

$$\begin{aligned} L^{(1)}\phi_{31} = A(t)(f^{\mathrm{iv}}_{11} - 2k^2 f''_{11} + k^4 f_{11}) + (dA/dt)(f''_{11} - k^2 f_{11}) \\ + A^2(t)\bar{A}(t)\{M(1, 0, f_{11}, f_{20}) + M(-1, 2, f_{1,-1}, f_{22})\} \end{aligned} \tag{3.23}$$

with the boundary conditions appropriate to a solution even in η. The operator $L^{(1)}$ does not involve $\partial/\partial t$, so that t is a parameter and (3.23) is an ordinary differential equation with η as the independent variable. Since the equation $L^{(1)} f = 0$ has the non-trivial solution $f = f_{11}$ with the same boundary conditions then (3.23) has a solution if and only if the integral of the product of the right-hand side with the adjoint eigenfunction is zero. We denote the adjoint eigenfunction by $v(\eta)$; the problem for $v(\eta)$ is

$$\left.\begin{aligned} (1/R_1)(v^{\mathrm{iv}} - 2k^2 v'' + k^4 v) &= ik\{(w - \lambda)(v'' - k^2 v) + 2w'v'\}, \\ v = v' = 0 \quad \text{at} \quad \eta = 1; \quad v &= v''' = 0 \quad \text{at} \quad \eta = 0. \end{aligned}\right\} \tag{3.24}$$

Then the solvability condition applied to (3.23) yields

$$dA/dt = aA + bA^2\bar{A}, \tag{3.25}$$

where

$$a = \frac{-\int_0^1 (f^{\mathrm{iv}}_{11} - 2k^2 f''_{11} + k^4 f_{11})\, v\, d\eta}{\int_0^1 (f''_{11} - k^2 f_{11})\, v\, d\eta}, \tag{3.26}$$

$$b = \frac{-\int_0^1 \{M(1, 0, f_{11}, f_{20}) + M(-1, 2, f_{1,-1}, f_{22})\}\, v\, d\eta}{\int_0^1 (f''_{11} - k^2 f_{11})\, v\, d\eta}. \tag{3.27}$$

It is interesting to notice that with this formulation of the problem the amplitude equation is exact. Higher order effects would be dealt with by introducing new amplitude functions as in Matkowsky (1970). The constant a depends only on the linear part of the problem, and if we expand the linear problem about $R = R_1$, $c = \lambda + i0$ it is easy to show that

$$-ikc = -ik\lambda + \epsilon^2 a + \dots . \tag{3.28}$$

We therefore know that the real part of a is positive, since it represents the part of c which causes growth for $R > R_1$ in the linear problem.

The constant b represents nonlinear effects. We have calculated this constant and found that its real part is positive, at least for some range of the parameters γ and k. Some numerical results will be presented later.

4. The limiting flow for large time

To obtain a differential equation for $|A(t)|^2$ we multiply (3.25) by $\bar{A}$ and add the result to the complex conjugate to obtain

$$d|A|^2/dt = k_1|A|^2 + k_2|A|^4, \tag{4.1}$$

where

$$k_1 = a + \bar{a} = 2a_r, \quad k_2 = b + \bar{b} = 2b_r, \tag{4.2}$$

a_r and a_i denote the real and imaginary parts of a, and similarly for b. Now for real ϵ ($R > R_1(k)$) we know that $a_r > 0$. If $b_r < 0$ it can easily be seen that

$$|A| \to (a_r/|b_r|)^{\frac{1}{2}} \quad \text{as} \quad t \to \infty. \tag{4.3}$$

It should be realized that the constant b, and the amplitude function $A(t)$, depend upon the normalization adopted for $f_{11}(\eta)$, although the final stream function is, of course, independent of this. If we multiply f_{11} by a constant K then f_{22} and f_{20} are multiplied by K^2, f_{31} is multiplied by K^3, b is multiplied by K^2, and $A(t)$ is multiplied by $1/K$. Let us now suppose that

$$\int_0^1 |f_{11}(\eta)|\, d\eta = 1. \tag{4.4}$$

Then we can see that with $a_r > 0$ and $b_r < 0$

$$\int_0^1 |A(t) f_{11}(\eta)|\, d\eta \to (a_r/|b_r|)^{\frac{1}{2}} \quad \text{as} \quad t \to \infty. \tag{4.5}$$

Therefore $\epsilon(a_r/|b_r|)^{\frac{1}{2}}$ is a measure of the size of the perturbation stream function and we shall expect the expansion to be useful if this quantity is small compared with the steady-state stream function.

Although $|A| \to$ constant as $t \to \infty$ it can easily be shown that $\arg\{A(t)\}$ does not. In fact

$$A(t) \to (a_r/|b_r|)^{\frac{1}{2}} \exp\{i(b_r a_i - b_i a_r)\, t/b_r\} \quad \text{as} \quad t \to \infty. \tag{4.6}$$

When we write the flow in terms of the original time variable τ we see that since $t = \epsilon^2 \tau$ the variation in the argument of $A(t)$ is an $O(\epsilon^2)$ effect. The stream function for the total flow becomes

$$\psi = \int^{\eta} w\, d\eta + 2\mathrm{Re}\{\epsilon(a_r/|b_r|)^{\frac{1}{2}} f_{11}(\eta)\, e^{ik(\xi - \lambda\tau)}\} + O(\epsilon^2) \tag{4.7}$$

for large values of the time.

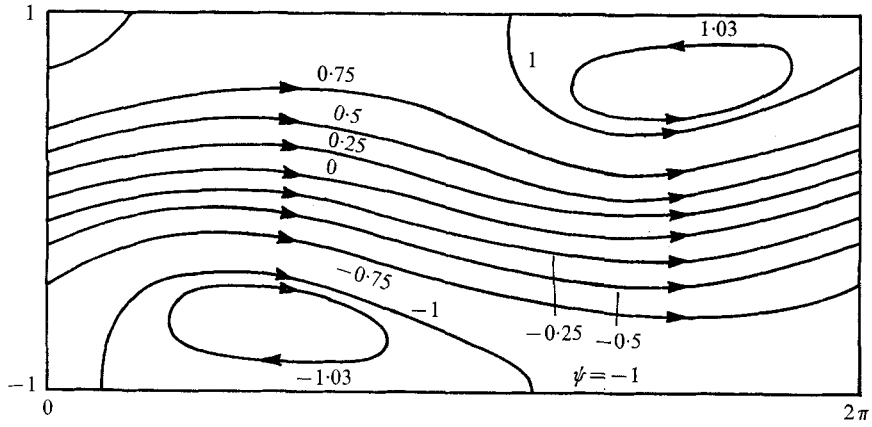

FIGURE 4. Streamlines of the secondary flow with τ fixed. The case illustrated is with $\gamma = 4{\cdot}71$, $\epsilon = 0{\cdot}162$, $R = 100$ and $\alpha = 0{\cdot}0475$. The co-ordinates ξ and η are defined in (2.1).

We have calculated the flow given by (4.7) for a number of cases, and a typical pattern is shown in figure 4. The case illustrated has very weak vortices. Stronger vortices are obtained with larger values of ϵ, i.e. at higher values of R. Such a flow might be realized if we gradually increased R and simultaneously decreased α, keeping $\gamma = R\alpha$ fixed, until R became slightly greater than $R_1(k)$, and then introduced a small disturbance like $f_{11}(\eta)\, e^{ikx}$. This should grow to give the flow pattern of figure 4.

It is possible that a more general disturbance might give a flow pattern of a similar type through the linear selection of the most unstable mode. In this case the most likely value of k is that which gives $R_1(k) = R_c$.

However, recent work by Stewartson & Stuart (1971) shows that the amplitude equation (3.25) should be modified for more general initial disturbances. Our amplitude equation is a special case of their more general equation.

5. The numerical work and some results

Fortunately we had some results for the neutral curves of the linear problem for various values of γ. These figures (unpublished) were tables of k, $R_1(k)$ and $c_r(k)$ on the neutral curves, calculated some years ago by a well-tested computer program (Eagles 1966). To find the linear eigenfunction $f_{11}(\eta)$ of problem (3.18) we used the appropriate values of R_1 and c_r for our chosen value of k. We then defined two integrals of (3.18):

$$U_1(\eta), \quad \text{satisfying} \quad U_1 = U_1' = U_1''' = 0, \quad U_1'' = 1 \quad \text{at} \quad \eta = 0; \tag{5.1}$$

$$U_2(\eta), \quad \text{satisfying} \quad U_2' = U_2'' = U_2''' = 0, \quad U_2 = 1 \quad \text{at} \quad \eta = 0. \tag{5.2}$$

We then chose the constants A and B in $AU_1(\eta) + BU_2(\eta) = f(\eta)$ to make $f(\eta)$ satisfy $f = 0$ at $\eta = 1$, and to satisfy (4.4). We checked that this then satisfied $f' = 0$ at $\eta = 1$. This provided a useful check on the calculations, for if either

R_1, or c_r, or the integrations had been in error we should have found $f'(1) \neq 0$ (except by an almost impossible cancellation of errors). It should be noted that, in these calculations, R_1 was not large enough to require us to use any special techniques. A straight-forward fourth-order Runge–Kutta scheme was found to be sufficiently accurate for values of $R_1 k$ up to about 200, at which value 48 Runge–Kutta steps gave an accuracy of about $3\frac{1}{2}$ significant figures. For lower values of $R_1 k$ the accuracy was much better.

Having found $f_{11}(\eta)$ we then proceeded to solve problems (3.20) and (3.22) for $f_{22}(\eta)$ and $f_{20}(\eta)$. These presented no difficulty. We combined two integrals of the homogeneous differential equation and a particular integral of the full differential equation, each satisfying the boundary conditions at $\eta = 0$, in order to satisfy the conditions at $\eta = 1$.

The adjoint problem (3.24) for $v(\eta)$ was solved and checked by the same method as that used for $f_{11}(\eta)$. The adjoint was also re-calculated in a separate program by using a matrix formulation of the adjoint problem, involving different integrations, to provide another check.

The constants a and b of (3.25), under the condition (4.4), were then found using Simpson's formula for integration. The results were obtained to an estimated accuracy of 3 significant figures (at worst), by taking 48 steps for the eigenfunction and 24 steps for $f_{20}(\eta)$ and $f_{22}(\eta)$.

As a further check on the results we replaced the operator $L^{(n)}$ by the operator

$$Q^{(n)} = \frac{d^4}{d\eta^4} + \beta^2 \frac{d^2}{d\eta^2}, \quad \beta = \frac{(3+n)\pi}{2(n+1)}. \tag{5.3}$$

For this operator one can calculate the functions f_{11}, f_{20} and f_{22} and the constants a and b analytically, starting with the linear eigenfunction $f_{11} = \cos \pi\eta + 1$. The results were found to agree with those from the computer program.

In table 1 we present a selection of the results for the constants, and in figure 2 we show some of the velocity profiles $w(\eta; \gamma)$. For the case $\gamma = 3{\cdot}07$ we calculated only one case, with $k = 2{\cdot}0$. This was because in this case we did not have the neutral-curve figures available from earlier work and considerable calculations were needed for each value of k. The value chosen is a little above the linear critical value.

At this point we shall discuss briefly the validity of the approximations. There are two distinct processes of approximation involved. One is replacing the exact partial differential equation (2.7) by the modified equation (2.10), by ignoring those terms in (2.7) which are formally of $O(\alpha)$ with $\gamma = R\alpha$ fixed, except that we retain $(1/R) D^4 \psi_1$. The other approximation is the use of series (3.7) as an approximation to a solution of (2.10). We think of the wavenumber k as fixed. The first approximation becomes better as α becomes smaller, that is as R becomes larger. The second approximation becomes better as ϵ becomes smaller, that is as R approaches $R_1(k)$ on the neutral curve appropriate to the linear version of (2.10). Thus the two processes are competing, for as one approximation becomes better the other becomes worse. However, if $R_1(k)$ is sufficiently large we shall expect both approximations to be good in the region $R_1(k) < R < \infty$. For the case illustrated ($\gamma = 4{\cdot}71$) we have chosen $k = 1{\cdot}934$, and then $R_1(k) = 27{\cdot}58$. We

k	R_1	λ	a_r	a_i	b_r	b_i	$(a_r/\|b_r\|)^{\frac{1}{2}}$
			$\gamma = 3{\cdot}07$, $R_c \doteq 80$				
2·000	83·40	0·9041	12·3	6·98	−45·0	−10·0	0·522
			$\gamma = 3{\cdot}57$, $R_c = 54{\cdot}7$				
2·284	67·96	0·9759	11·8	5·28	−54·0	−0·620	0·468
1·833	54·68	0·8628	13·6	1·39	−37·4	0·246	0·602
1·383	65·65	0·7000	13·3	−0·58	−20·2	−2·17	0·812
			$\gamma = 4{\cdot}71$, $R_c = 27{\cdot}6$				
2·944	52·09	1·147	12·1	0·300	−76·6	45·9	0·399
1·934	27·58	0·853	14·4	−2·04	−32·5	3·42	0·665
0·9655	50·75	0·349	11·6	−4·91	−7·92	−3·70	1·21
			$\gamma = 5{\cdot}10$, $R_c = 20{\cdot}8$				
3·087	35·84	1·2062	1·52	−0·764	−75·3	49·1	0·449
2·082	20·83	0·8831	1·49	−2·39	−33·1	4·83	0·671
0·8905	41·01	0·1624	1·12	−5·74	−6·11	−3·85	1·36
			$\gamma = 5{\cdot}45$, $R_c = 12{\cdot}8$				
3·582	29·47	1·436	19·0	−5·17	−94·6	91·7	0·448
2·083	12·80	0·7992	15·1	−3·29	−24·7	24·7	0·779
1·334	15·92	0·1910	12·6	−5·09	−9·87	−3·26	1·13

TABLE 1. The values of the constants a and b, which are defined in (3.25)–(3.27), and the values of the equilibrium amplitude $(a_r/|b_r|)^{\frac{1}{2}}$. These constants were calculated with $f_{11}(\eta)$ normalized according to (4.4). For the given value of k, $R_1(k)$ is the Reynolds number on the neutral curve and $\lambda(k)$ is the real part of the linear eigenvalue c on the neutral curve.

have chosen $R = 100$ and thus $\epsilon = 0{\cdot}162$ and $\alpha = 0{\cdot}0475$. In this case we checked the computed figures and found that typical terms like $\alpha\,\partial^2\psi_1/\partial\eta^2$ are indeed small compared with the terms retained. For example, near $\eta = 1$,

$$\alpha|\partial^2\phi_{11}/\partial\eta^2| = 0{\cdot}85, \quad \text{while} \quad (1/R_1)\,|\partial^4\phi_{11}/\partial\eta^4| = 18.$$

However, in obtaining (2.10) we also replaced $e^{2\alpha\xi}\,\partial/\partial\tau$ by $\partial/\partial\tau$. This requires that $e^{2\alpha\xi}$ should not vary too much over a wavelength $2\pi/k$. We have $(2\alpha)\,(2\pi/k) = 0{\cdot}30$ so the requirement is reasonably satisfied. At the same time $\epsilon = 0{\cdot}162$ is sufficiently small. By taking cases of smaller γ we would find larger $R_1(k)$ near R_c, and so even better cases for application. However, computational difficulties arise because of the large values of R_1 involved, and such calculations were not attempted.

We found the pattern of figure 4 typical for values of γ between 3·07 and 5·45, but our approximation is of doubtful value for the higher values of γ since α becomes rather too large. On the other hand, we were unable to calculate streamlines for smaller values of γ because R_c becomes so large that special techniques are needed for solving the differential equations, and our simple program would not work. We were therefore unable to make a direct check with the results of Reynolds & Potter (1967) for Poiseuille flow ($\gamma = 0$), that b_r is positive over most of the neutral curve, but negative on the lower branch for large values of R.

Appendix. The Jeffery–Hamel velocity profiles

The velocity profiles $w(\eta;\gamma)$ used in this work are conveniently obtained by specifying the parameter m, which first decreases from 1 to 0·5 and then increases again to 0·57, and then finding b as the solution of

$$3m\,\mathrm{cn}^2(b|m) = 2m - 1 \tag{A 1}$$

in such a way that $\mathrm{cn}(b|m)$ increases as m varies as described above, while $0 \leqslant b \leqslant 2K$. Then with

$$\rho = E(b|m) - b\,dn^2(b|m) \tag{A 2}$$

we find that

$$\gamma = 6b\rho \tag{A 3}$$

and

$$w(\eta;\gamma) = (mb/\rho)\{\mathrm{sn}^2(b|m) - \mathrm{sn}^2(b\eta|m)\}. \tag{A 4}$$

These are the JHII family members; see Fraenkel (1962) for further details. The parameter m is the square of the usual modulus, $\mathrm{sn}(b|m)$ etc. are the usual Jacobean elliptic functions of modulus $\sqrt{m}$, and K is the quarter-period.

I should like to thank Professor J. T. Stuart for several helpful discussions and to acknowledge the help of the computing advisory service at The City University.

REFERENCES

EAGLES, P. M. 1966 *J. Fluid Mech.* **24**, 191–207.

EAGLES, P. M. 1969 *Quart. J. Mech. Appl. Math.* **22**, 183–210.

FRAENKEL, L. E. 1962 *Proc. Roy. Soc.* A **267**, 119–136.

FRAENKEL, L. E. 1963 *Proc. Roy. Soc.* A **272**, 406–428.

LIN, C. C. 1955 *The Theory of Hydrodynamic Stability*. Cambridge University Press.

MATKOWSKY, B. J. 1970 *SIAM J. Appl. Math.* **18**, 872–883.

PEKERIS, C. L. & SHKOLLER, B. 1967 *J. Fluid Mech.* **29**, 31–38.

REYNOLDS, W. C. & POTTER, M. C. 1967 *J. Fluid Mech.* **27**, 465–492.

STEWARTSON, K. & STUART, J. T. 1971 *J. Fluid Mech.* **48**, 529–545.

STUART, J. T. 1960 *J. Fluid Mech.* **9**, 353–370.

WATSON, J. 1960 *J. Fluid Mech.* **9**, 371–389.